J Membrane Biol (2008) 223:73–85
DOI 10.1007/s00232-008-9115-7

Na^+ Modulates Anion Permeation and Block of $P2X_7$ Receptors from Mouse Parotid Glands

Juan Pablo Reyes · Patricia Pérez-Cornejo · Carmen Y. Hernández-Carballo · Alaka Srivastava · Victor G. Romanenko · Mireya Gonzalez-Begne · James E. Melvin · Jorge Arreola

Received: 22 February 2008 / Accepted: 16 May 2008 / Published online: 1 July 2008

Abstract We previously reported that mouse parotid acinar cells display anion conductance (I_{ATPCl}) when stimulated by external ATP in Na^+-free extracellular solutions. It has been suggested that the $P2X_7$ receptor channel ($P2X_7R$) might underlie I_{ATPCl}. In this work we show that I_{ATPCl} can be activated by ATP, ADP, AMP-PNP, ATPγS and CTP. This is consistent with the nucleotide sensitivity of $P2X_7R$. Accordingly, acinar cells isolated from $P2X_7R^{-/-}$ mice lacked I_{ATPCl}. Experiments with $P2X_7R$ heterologously expressed resulted in ATP-activated currents ($I_{ATP\text{-}P2X7}$) partially carried by anions. In Na^+-free solutions, $I_{ATP\text{-}P2X7}$ had an apparent anion permeability sequence of $SCN^- > I^- \cong NO_3^- > Br^- > Cl^- >$ acetate, comparable to that reported for I_{ATPCl} under the same conditions. However, in the presence of physiologically relevant concentrations of external Na^+, the Cl^- permeability of $I_{ATP\text{-}P2X7}$ was negligible, although permeation of Br^- or SCN^- was clearly resolved. Relative anion permeabilities were not modified by addition of 1 mM carbenoxolone, a blocker of Pannexin-1. Moreover, cibacron blue 3GA, which blocks the Na^+ current activated by ATP in acinar cells but not I_{ATPCl}, blocked $I_{ATP\text{-}P2X7}$ in a dose-dependent manner when Na^+ was present but failed to do so in tetraethylammonium containing solutions. Thus, our data indicate that $P2X_7R$ is fundamental for I_{ATPCl} generation in acinar cells and that external Na^+ modulates ion permeability and conductivity, as well as drug affinity, in $P2X_7R$.

Keywords Salivary gland · $P2X_7$ receptor · Anion permeability · Fluid secretion · ATP · Na^+

J. P. Reyes · C. Y. Hernández-Carballo · J. Arreola (✉)
Instituto de Física, Universidad Autónoma de San Luis Potosí, Dr. Manuel Nava #6, San Luis Potosi SLP 78290, Mexico
e-mail: arreola@dec1.ifisica.uaslp.mx

P. Pérez-Cornejo
Facultad de Medicina, Universidad Autónoma de San Luis Potosí, San Luis Potosi SLP 78290, Mexico

A. Srivastava · V. G. Romanenko · M. Gonzalez-Begne · J. E. Melvin
Center for Oral Biology, University of Rochester Medical Center, Rochester, NY 14642, USA

J. Arreola
Pharmacology and Physiology Department, University of Rochester Medical Center, Rochester, NY 14642, USA

Introduction

Adenosine 5′-triphosphate (ATP) acts as an external signaling molecule in a variety of tissues (for reviews, see North 2002; Burnstock 2007). Many of the cellular responses to external ATP are mediated by activation of G protein–coupled metabotropic P2Y and/or ionotropic P2X purinoceptors present in the plasma membrane of cells in numerous tissues (Burnstock 2007; North and Barnard 1997; Ralevic and Burnstock 1998). Epithelial cells express both P2Y and P2X receptors (Tenneti et al. 1998; Fukushi 1999; Schwiebert and Zsembery, 2003; Li et al. 2003; Hayashi et al. 2005; Ma et al. 2006). While the detailed physiological role of these receptors remains unclear, it has been shown that external ATP induces multiple cellular events important to the functions of epithelia (Roman and Fitz 1999; Leipziger 2003). For example, external ATP increases both cationic and anionic conductances in the plasma membrane of epithelial cells (Leipziger 2003; Li et al. 2005; Arreola and Melvin 2003). Specifically, activation of P2Y receptors generates a G protein–coupled increase in inositol 1,4,5-triphosphate

($InsP_3$) that leads to Ca^{2+} release from intracellular stores, while activation of P2X receptor channels directly mediates Na^+ and Ca^{2+} entry (for a complete review, see Burnstock 2007). The resulting increase in $[Ca^{2+}]_i$ associated with activation of either class of P2 receptors is likely to be important for epithelial fluid secretion since Ca^{2+} induces opening of Ca^{2+}-dependent Cl^- and K^+ channels, which are key to initiating and sustaining fluid and electrolyte secretion (Melvin et al. 2005).

Salivary acinar cells express at least four different types of purinoceptors, $P2Y_1$ and $P2Y_2$ as well as $P2X_4$ and $P2X_7$ (Turner et al. 1999; Li et al. 2003), whose stimulation results in an increase in intracellular Ca^{2+} (McMillan et al. 1993). Although the physiological role of $P2X_4$ and $P2X_7$ ionotropic receptors expressed in these cells remains unknown, it has been shown that stimulation of exocrine gland acinar cells with external ATP activates Ca^{2+}-dependent ion currents (Li et al. 2003) including those associated with Ca^{2+}-dependent Cl^- channels. Additionally, in mouse parotid acinar cells bathed in Na^+-free medium, external ATP activates a Ca^{2+}-independent anion conductance named I_{ATPCl} (Li et al. 2005; Arreola and Melvin 2003). We found that the kinetics and channel pharmacology of I_{ATPCl} are different from other anion channels previously described in salivary gland acinar cells, including the Ca^{2+}-dependent, ClC-2, CFTR and volume-sensitive Cl channels (Arreola and Melvin 2003; Zeng et al. 1997). Moreover, the P2X receptor antagonist cibacron blue 3GA (CB) did not block I_{ATPCl} when recorded in solutions containing tetraethylammonium chloride (TEACl) and 0 Na^+. In contrast, CB blocks the ATP-activated Na^+ current presumably flowing through P2X receptors (Arreola and Melvin 2003). Thus, we suggested that I_{ATPCl} has an anion conductance component with novel characteristics, including more sensitivity to Bz-ATP than ATP and resistance to the P2X receptor antagonist CB. Recently, Li et al. (2005), using acinar and duct cells from parotid glands of wild-type and $P2X_7R^{-/-}$ mice, suggested that I_{ATPCl} results from regulation of $P2X_7R$ by external Cl^- and Na^+. They also concluded that $P2X_7R$ is not permeable to Cl^-. This study prompted us to further investigate the role of $P2X_7R$ in the generation of I_{ATPCl} using a pharmacological approach and $P2X_7R^{-/-}$ mice. In addition, recombinant mouse $P2X_7R$ cloned from parotid acinar cells was used to determine if the resulting ATP-activated currents ($I_{ATP\text{-}P2X7}$) displayed anion permeability sensitive to CB and extracellular Na^+ similar to I_{ATPCl}. Our data show that $P2X_7R$ is essential for I_{ATPCl} generation and that $I_{ATP\text{-}P2X7}$ has indeed anion permeability similar to that of I_{ATPCl} and conductivity which is modulated by extracellular Na^+. Furthermore, CB blocks $P2X_7R$ when Na^+ is present but in the absence of external Na^+ CB potentiates the current through the receptor. Thus, our data indicate that $P2X_7R$ is fundamental for I_{ATPCl} generation and that the functional structure of $P2X_7R$ may be critically dependent on external Na^+.

Materials and Methods

$P2X_7R^{-/-}$ Mice

$P2X_7R^{-/-}$ mice were kindly provided by Dr. Christopher A. Gabel (Pfizer Global Research and Development, Groton, CT) (Solle et al. 2001) and bred at the University of Rochester's vivarium. Wild-type (WT) C57BL/6J (Jackson Laboratories, Bar Harbor, ME) and $P2X_7R$ null mice aged 2–6 months were used following protocols approved by the Animal Resources Committee of the University of Rochester.

Cloning of $P2X_7R$ and $P2X_4R$ from Mouse Parotid Gland

Total RNA was isolated from mouse parotid gland (RNEASY Mini Kit; Qiagen, Valencia, CA) followed by DNAse treatment. First-strand cDNA was synthesized from total RNA using the ISCRIPT cDNA synthesis kit (Bio-Rad, Hercules, CA). Full-length cDNAs were amplified by polymerase chain reaction (PCR) using the following gene-specific primers: $P2X_7R$ (accession NM_011027) 5′-GAA TTC GGC TTA TGC CGG CTT GCT GC-3′, 5′-CGG CTT TCA GTA GGG ATA CTT GAA GCC-3′ and $P2X_4R$ (accession AF089751) 5′-CAT TAG AAT TCA CGA GGC GGA CGA GC-3′, 5′-CGA GAG AAT TCG GTT AGG CAT CAC TGG TC-3′.

PCR products were isolated (PCR cleaning kit, Qiagen) and their sequences verified. The 5′ and 3′ untranslated regions of $P2X_7R$ and $P2X_4R$ contained *Eco*RI sites to facilitate insertion of each clone into a bicistronic expression vector (pIRES2-EGFP; Clontech, Palo Alto, CA), generating pIRES2-EGFP-$P2X_7R$ and pIRES2-EGFP-$P2X_4R$ vectors, respectively. In addition, the mouse $P2X_7R$ clone was inserted in an inverted fashion (pIRES2-EGFP-$P2X_7R_{inv}$) into the pIRES2-EGFP vector as a negative control. The cDNA sequences obtained for mouse parotid $P2X_7R$ and $P2X_4R$ were identical to those previously published in the NCBI database.

Biotinylation of Cell Surface Proteins

Biotinylation of cell surface proteins was performed according to the manufacturer's instructions (Pierce Biotechnology-Thermo Fisher Scientific Inc; Rockford, IL). Parotid acinar cells were prepared as previously described (Evans et al. 1999). Briefly, $C57Bl/6J^{+/+}$ are from now on referred to as wild type (WT) and $P2X7^{-/-}$ mice were

rendered unconscious by exposure to CO_2 and killed by exsanguination prior to isolation of cells by collagenase digestion. Dispersed cells were washed twice with ice-cold phosphate-buffered saline (PBS, pH 8.0) prior to addition of 80 μl of 10 mM Sulfo NHS-SS-Biotin (Pierce Biotechnology-Thermo Fisher Scientific Inc; Rockford, IL) stock solution per milliliter of PBS. After 30 min at room temperature (22°C), the reaction was stopped by addition of ice-cold 50 mM Tris (pH 8.0) for 10 min, and then the cells were washed twice with ice-cold PBS.

Preparation of Crude and Affinity-Enriched Plasma Membrane Proteins

Biotinylated cells were collected by centrifugation at 1,000 × *g* for 45 s, and the pellet was resuspended in 5 ml of ice-cold homogenizing buffer containing 250 mM sucrose (J. T. Baker, Philipsburg, NJ), 10 mM TEA, leupeptin (1 μg/ml) and phenylmethanesulfonyl fluoride (0.1 mg/ml). Cells were homogenized with the ULTRA TURRAX T8 Homogenizer (IKA, Werke, Germany). Unbroken cells and nuclei were pelleted at 4,000 × *g* for 10 min at 4°C. The supernatant was saved and the pellet resuspended and centrifuged in the same volume of homogenization buffer as before. The collected supernatants were pooled and centrifuged at 22,000 × *g* for 20 min at 4°C. The pellet was suspended in the same buffer and centrifuged at 46,000 × *g* (Beckman SW28 rotor; Beckman Coulter; Fullerton, CA) for 30 min at 4°C. The resultant crude pellet was resuspended in 1 ml of hypotonic buffer containing 10 mM HEPES (pH 7.5), 1.5 mM $MgCl_2$, 10 mM KCl, Complete Protease Inhibitor Cocktail (1 tablet/50 ml; Roche Applied Science, Indianapolis, IN), 1 mM Na_3VO_4 and 1 mM NaF, then incubated with 200 μl of Dynabeads M-280 streptavidin (Dynal Biotech, Oslo, Norway) at 4°C overnight. Beads were collected with a magnetic plate and washed with hypotonic buffer to obtain the membrane-associated fractions. The streptavidin beads carrying the enriched plasma membrane fractions were suspended in 100 mM dithiothreitol for 2 h according to the manufacturer's instructions and then centrifuged at 10,600 × *g* for 3 min. The supernatants were collected and used for electrophoretic analysis.

Electrophoresis and Western Blot Analysis

Protein (50 μg) was heated at 95°C for 5 min prior to separation in a 7.5% or 10% sodium dodecyl sulfate-polyacrylamide gel electrophoresis (SDS-PAGE) Tris-glycine mini-gel (Bio-Rad). Protein was transferred onto polyvinylidene difluoride (PVDF) membranes (Invitrogen, Carlsbad, CA) overnight at 4°C using a transfer buffer containing 10 mM 3-[cyclohexylamino]-1-propanesulfonic acid (CAPS, pH 11) in 10% methanol. Membranes were blocked overnight at 4°C with 5% nonfat dry milk in 25 mM Tris-HCl (pH 7.5), 150 mM NaCl (TBS) and then incubated with primary antibody for $P2X_7R$ (Millipore-Chemicon, Temecula, CA) at a dilution of 1:300 in 2.5% nonfat dry milk solution at 4°C overnight. After washing with TBS containing 0.05% Tween-20 (TBS-T), the membranes were incubated with horseradish peroxidase–conjugated goat anti-rabbit IgG secondary antibody (Pierce) at a dilution of 1:2,500 in TBS-T/2.5% nonfat dry milk for 1 h at room temperature. Labeled proteins were visualized using enhanced chemiluminescence (ECL detection kit; GE-Amersham Biosciences, Piscataway, NJ).

Single Parotid Acinar Cell Isolation

Single acinar cells were isolated from WT or $P2X_7R^{-/-}$ parotid glands as previously described (Arreola et al. 1995). Briefly, glands were dissected from exsanguinated mice under CO_2 anesthesia and minced in Ca^{2+}-free minimum essential medium (MEM; GIBCO BRL, Gaithersburg, MD) supplemented with 1% bovine serum albumin (BSA, Fraction V; Sigma, St. Louis, MO). The tissue was treated for 20 min (37°C) in MEM Ca^{2+}-free solution containing 0.02% trypsin + 1 mM EDTA (ethylenediaminetetraacetic acid) + 2 mM glutamine + 1% BSA. Digestion was stopped with 2 mg/ml of soybean trypsin inhibitor (Sigma), and the tissue was further dispersed by two sequential treatments of 60 min each with collagenase (0.04 mg/ml; Boehringer Mannheim, Indianapolis, IN) in MEM-Ca^{2+}-free + 2 mM glutamine + 1% BSA. Dispersed cells were centrifuged and washed with basal medium Eagle (BME, GIBCO BRL). The final pellet was resuspended in BME + 2 mM glutamine, and cells were plated onto poly-L-lysine-coated glass coverslips for electrophysiological recordings.

Culture and Transient Transfection of HEK-293 Cells

HEK-293 cells (Invitrogen) were maintained in Dulbecco's modified Eagle medium (DMEM, GIBCO BRL) at 37°C in a 95% O_2/5% CO_2 atmosphere. Cells were grown on 30-mm Petri dishes to 50–60% confluence and then transfected with either pIRES2-EGFP-$P2X_7R$, pIRES2-EGFP-$P2X_4R$ or pIRES2-EGFP-$P2X_7R_{Inv}$ DNA (2 μg/dish of a 1 μg/μl stock) according to the manufacturer's instructions using Polyfect transfection reagents (Qiagen). Transfected cells were detached from culture dishes using trypsin, plated onto 5-mm glass coverslips and allowed to reattach for at least 5 h before use.

Electrophysiological Recordings

A single coverslip containing either freshly isolated mouse parotid acinar or transfected HEK-293 cells was placed in a recording chamber mounted on the stage of a Nikon

(Tokyo, Japan) inverted fluorescence microscope equipped with ultraviolet (UV) illumination. Enhanced green fluorescent protein (EGFP) fluorescence observed under blue light (~488 nm) illumination was used to identify transfected HEK-293 cells.

Currents were recorded at room temperature (20–22°C) using the conventional whole-cell patch-clamp configuration (Hamill et al. 1981) and an Axopatch 200B amplifier (Axon Instruments, Foster City, CA). Pipettes made with Corning 8161 glass (Warner Instruments, Hamden, CT) have a resistance of 3–4 MΩ when filled with pipette solutions. The standard pipette (internal) solution contained (in mM) TEA^+ (or Na^+) Cl 140, EGTA 20 and HEPES 20 (pH 7.3, tonicity was ~335 mosm/kg). Cells were bathed in a standard external solution containing (in mM) TEA^+ (or Na^+) Cl 140, $CaCl_2$ 0.5, D-mannitol 100 and HEPES 20 (pH 7.3, tonicity was ~375 mosm/kg). A 3 M KCl agar bridge was used to ground a 300-µl recording chamber. The internal solution was Ca^{2+}-free, while the external was hypertonic to preclude activation of Ca^{2+}-dependent and volume-sensitive chloride currents, respectively, which are endogenous to mouse parotid acinar and HEK-293 cells (Pérez-Cornejo and Arreola 2004; Hernandez-Carballo et al. 2003). Tonicity of the solutions was determined using a vapor pressure osmometer (Wescor, Logan, UT).

Voltage ramps (from –100 to +100 mV in 1 s, every 2.5 s) were used to generate *I–V* curves and to estimate reversal potentials. To determine P_{TEA}/P_{Cl} or P_{Na}/P_{Cl}, the external solutions were prepared as above with absolute TEACl or NaCl concentrations equal to (in mM) 35, 50, 70, 100 and 140 or 27, 53, 73, 93, 113, 133 and 153, respectively (internal [TEACl] or [NaCl] was fixed at 141 mM using the standard internal solutions). To assay the effects of external $[Na^+]$ on $I_{ATP\text{-}P2X7}$ Br^- or SCN^- permeation, a mole fraction experiment was performed in cells dialyzed with the standard TEA^+ internal solution while keeping the total external cation concentration $(Na^+ + TEA^+) = 140$ mM. In these experiments, the pH of the external solution was adjusted to 7.3 with 20 mM HEPES, 0.5 mM $CaCl_2$ was present and tonicity was adjusted to ~375 mosm/kg with D-mannitol. To determine the anion permeation of $I_{ATP\text{-}P2X7}$, Cl^- was substituted with equimolar concentrations of SCN^-, I^-, NO_3^-, Br^- or acetate (supplied as TEA salts) in the standard external solution.

ATP, cytosine 5′-triphosphate (CTP), guanosine 5′-triphosphate (GTP), uridine 5′-triphosphate (UTP), adenosine 5′-diphosphate (ADP), adenosine 5′-monophosphate (AMP), adenosine (A), ATPγS, AMP-PNP and TNP-ATP were added to the external solution at a final concentration of 5 mM, whereas P3-[1-(2-nitrophenyl)]ethyl ester of ATP (NPE-caged ATP) was added to a final concentration of 250 µM. After nucleotide addition, the solution pH was readjusted to 7.3 with TEAOH or NaOH. Block of $I_{ATP\text{-}P2X7}$ by CB in the presence or absence of Na^+ was evaluated, constructing dose–response curves at +80 and –80 mV. Solutions were gravity-perfused at a flow rate of about 4 ml/min. Uncaging ATP was achieved by controlled photolysis using a pulsed xenon arc lamp (TILL Photonics, Eugene, OR) equipped with a fiber-optic guide. The fiber-optic guide was fed into an epifluorescence condenser attached to an inverted microscope. High-intensity (80 J) 1-ms flashes of UV light (~360 nm) were applied to release the ATP.

Voltage commands were delivered from a holding potential of 0 mV. Data were acquired using the software Clampex 9.0 (Axon Instruments). Unless otherwise indicated, data were filtered at 5 kHz and sampled at 10 kHz.

Analysis

The anion permeability sequence of P2X$_7$R was determined by performing standard protocols of ion substitution to determine reversal potential (E_r) shifts. These E_r values were plugged into the Goldman, Hodgkin and Katz (GHK) equation to estimate the apparent permeability of each anion relative to Cl^-. This technique has been extensively applied to determine selectivity of ion channels (Hille 2001). Since the purinoceptor channel is mainly permeable to cations (North 2002; Coutinho-Silva and Persechini 1997; Duan et al. 2003), we first determined the relative permeability of the major cations present in our external recording solutions (TEA^+ and Na^+) relative to Cl^- and subsequently used these values to determine an apparent permeability ratio to different anions.

P_{TEA}/P_{Cl} and P_{NA}/P_{Cl} ratios were separately determined by analyzing the effects of different external [TEACl] (with internal [TEA] = 141 mM) or different external [NaCl] (with internal [NaCl] = 141 mM), on the raw reversal potentials using the GHK equation:

$$E_r = \frac{RT}{F} \ln \frac{P_C[C^+]_e + P_{Cl}[Cl^-]_i}{P_C[C^+]_i + P_{Cl}[Cl^-]_e} \quad (1)$$

where $[C^+]_e$ and $[C^+]_i$ represent the external and internal concentrations of either $[TEA^+]$ or $[Na^+]$; P_C and P_{Cl} represent TEA or Na and Cl permeabilities, respectively; and *R, T* and *F* have their usual thermodynamic meanings.

Next, using the reversal potential shifts (ΔE_r) induced by replacing Cl^- in the standard external solution with anion X and the P_{TEA}/P_{Cl} determined from Eq. 1, an apparent permeability ratio for each anion relative to Cl^- (P_x/P_{Cl}) was estimated using another form of the GHK equation:

$$\Delta E_r = -\frac{RT}{F} \ln \frac{\frac{P_{TEA}}{P_{Cl}}[TEA^+]_i + \frac{P_x}{P_{Cl}}[X^-]_e}{\frac{P_{TEA}}{P_{Cl}}[TEA^+]_i + [Cl^-]_e} \quad (2)$$

where $[TEA^+]_i$ is the intracellular $[TEA^+] = 141$ mM; $[X^-]_e$ is the external SCN^-, I^-, NO^-_3, Br^- or acetate

concentration (140 mM); and $[Cl^-]_e = 140$ mM. Thus, these apparent permeability ratios would be valid only for 141 mM internal TEACl conditions. Measurements of E_r were also carried out in the presence of 1 mM carbenoxolone (CBX). CBX was dissolved in water and then added to the extracellular solution. In these experiments the cells were first preincubated for 5 min with CBX and CBX was present throughout the experiment.

Liquid junction potentials (LJPs) were measured for the standard external TEACl solution and for TEA solutions where Cl^- was substituted by SCN^-, I^-, NO_3^-, Br^- or acetate (Table 1). Membrane potential values were not corrected by LJP, and the resulting selectivity sequence estimated as described above was not altered by LJP.

Dose–response curves for ATP, ADP and CB blockade in the presence of Na^+ were fitted to a Hill equation:

$$\text{Response} = \frac{R_{max} - R_{min}}{\left(\frac{EC_{50}}{[A]}\right)^n + 1} + R_{min} \quad (3)$$

$$\text{Block} = \frac{R_{max} - R_{min}}{\left(\frac{[CB]}{IC_{50}}\right)^n + 1} + R_{min}$$

where R_{max} and R_{min} are the maximum and minimum percentages of response or block, [A] is either external ATP or ADP concentration, [CB] is CB concentration, EC_{50} and IC_{50} are [A] or [CB] to get 50% of maximum response or block and n is the Hill coefficient.

Experimental data are presented as the mean ± SEM. EC_{50}, IC_{50} and n values were obtained from fitting average data, and no errors are given. The statistical significance between groups was evaluated applying one-way analysis of variance and the post-hoc Scheffé test ($P < 0.05$).

Materials

Chemicals were obtained from Sigma, including $(Tris)_2$ and Na_2 salts of CTP, UTP, GTP, ATP, ADP, AMP, adenosine, ATPγS, AMP-PNP, TNP-ATP, NPE-caged ATP and CBX, unless indicated otherwise in the text.

Results

Pharmacology of I_{ATPCl} and $I_{ATP\text{-}P2X7}$

We have previously shown that ATP or Bz-ATP stimulation of voltage-clamped single parotid acinar cells (dialyzed and bathed in TEA^+-containing solutions with 0 Na^+) induces the appearance of a Ca^{2+}-independent ion current (referred to as I_{ATPCl}) that is partially carried by anions (Arreola and Melvin 2003). We suggested that I_{ATPCl} resulted from activation of a novel Cl^- conductance in parotid acinar cells, although recent data indicate that the ATP-activated currents, including I_{ATPCl}, are due to activation of cation-selective P2X$_7$ receptors (Li et al. 2005). This prompted us to further evaluate the role of P2X$_7$R in the generation of I_{ATPCl}. We reasoned that if P2X$_7$Rs are responsible for I_{ATPCl}, then both currents, I_{ATPCl} and $I_{ATP\text{-}P2X7}$ (current through P2X$_7$R expressed in HEK-293 cells and activated by ATP), should have similar pharmacological sensitivity and ion permeability characteristics.

Table 1 Apparent anion permeability of $I_{ATP\text{-}P2X7}$

Anion	E_r (mV) without CBX	E_r (mV) with 1 mM CBX	P_X/P_{Cl} without CBX	Liquid junction potential (mV)
SCN^-	−17.69 ± 0.49	−19.01 ± 1.52	7.31 ± 0.14	−1
	$n = 11$	$n = 6$		
I^-	−8.69 ± 0.46	−8.17 ± 0.79	3.28 ± 0.16	−1.3
	$n = 11$	$n = 6$		
NO_3^-	−7.46 ± 0.40	ND	2.83 ± 0.16	+1.5
	$n = 11$			
Br^-	−4.77 ± 0.47	ND	1.97 ± 0.15	−0.3
	$n = 10$			
Cl^-	−1.75 ± 0.22	−3.05 ± 0.86	1	−0.6
	$n = 12$	$n = 6$		
Acetate	+5.18 ± 0.86	+12.22 ± 3.57	~0.0 ± 0.00	+2.9
	$n = 10$	$n = 6$		

Shifts in reversal potential induced by anion substitution in Na^+-free, TEA-containing solutions were used with Eq. 2 to determine P_X/P_{Cl}. The term P_{TEA}/P_{Cl}, which is present in Eq. 2, was determined from the data in Fig. 4 as described in the text. Liquid junction potentials are listed for different anion substitution solutions. The −0.6 mV listed in the Cl^- row is the potential measured upon returning to the standard external solution after the anion substitution measurement

E_r, reversal potential of the current; n, number of cells tested; ND, not determined

The ability of a wide variety of nucleotides and ATP derivatives to activate I_{ATPCl} was tested by application of a single concentration (5 mM). A summary of these responses is presented in Fig. 1A, B, which shows representative raw traces obtained at +80 and −80 mV from a single acinar cell bathed in a standard external solution containing either 0 or 5 mM of the indicated nucleotides or ATP derivatives. I_{ATPCl} was readily activated by ATP and partially by CTP (Fig. 1A). Other nucleotides like GTP and UTP did not significantly activate the current. Raw traces in Fig. 1B show that ADP was the only ATP derivative which activated I_{ATPCl}, while AMP and adenosine failed to activate the current. Since ADP was able to activate I_{ATPCl}, we investigated whether metabolization of ATP to ADP was necessary for I_{ATPCl} activation. Figure 1C shows that AMP-PNP and ATPγS, two nonhydrolyzable ATP analogues, were able to activate I_{ATPCl}. Hence, ATP hydrolysis is not required for I_{ATPCl} activation. As expected, the antagonist TNP-ATP failed to activate the current. To further support the idea that ATP per se activates I_{ATPCl}, the external [ATP] was rapidly increased by applying UV light flashes to an extracellular solution containing 250 μM NPE-caged ATP. Figure 1C (rightmost traces) shows that a single UV flash (double-headed arrow) applied in the absence of caged ATP did not activate I_{ATPCl} (flat trace). However, addition of 250 μM NPE-caged ATP (arrowheads) to the same cell resulted in current activation (stair-like trace) after application of UV flashes. Collectively, these results suggest that ATP per se is sufficient to activate I_{ATPCl}.

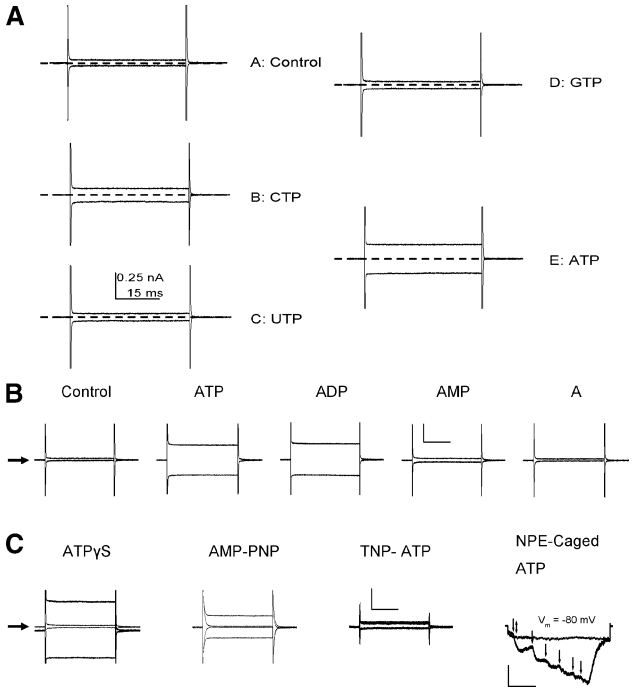

Fig. 1 Activation of I_{ATPCl} by trisphosphate nucleotides and ATP derivatives. (**A**) Raw current traces obtained from a single representative acinar cell stepped during 50 ms to −80 or +80 mV in the absence (control) or presence of 5 mM CTP, UTP, GTP or ATP. All currents were recorded using a standard internal solution that contained (in mM) 140 TEACl, 20 EGTA and 20 HEPES (pH 7.3), while the external solution contained (in mM) 140 TEACl, 0.5 $CaCl_2$, 100 D-mannitol and 20 HEPES (pH 7.3). *Dotted lines* indicate zero current level. (**B**) Raw traces recorded from a representative single acinar cell ($n = 5$) stepped for 50 ms to −80 and +80 mV in the absence (control) or presence of 5 mM ATP, ADP, AMP and adenosine (A). Calibration bars = 0.5 nA, 15 ms. (**C**) Representative traces obtained in the absence (traces of smaller amplitude) and in the presence of 5 mM of the nonhydrolyzable ATP analogues ATPγS ($n = 3$) and AMP-PNP ($n = 3$) and of 5 mM of the P2 receptor blocker TNP-ATP ($n = 3$). The slight shift from 0 current level in ATPγS was the result of using $(Na^+)_2$-ATP salt to activate the current. Calibration bars = 0.5 nA, 15 ms. *NPE-caged ATP*, Representative traces of a single cell stepped to −80 mV ($n = 4$). *Flat trace*, The cell was initially exposed to a short UV flash (*double-headed arrow*) in the absence of NPE-caged ATP (no response), then exposed to 250 μM NPE-caged ATP (no response). *Stair-like trace*, UV flashes (*arrows*) were applied in the presence NPE-caged ATP. Current returned to control level by perfusing the bath with the standard external solution. Calibration bars = 0.1 nA, 10 ms. *Arrows on the left* indicate zero current levels in all cases

Our previous dose–response experiments done using 0 Na^+, TEA^+-containing solutions showed that ATP activates I_{ATPCl} in acinar cells with an EC_{50} of 158 ± 10 μM and a Hill coefficient of 3.4 ± 0.4 at +80 mV (Arreola and Melvin 2003). Data in Fig. 1A show that ADP was able to activate I_{ATPCl}. Consequently, we carried out whole-cell recordings under the same experimental conditions with $P2X_7R$ cloned from the mouse parotid gland and expressed in HEK-293 cells to test the ability of external ATP and ADP to activate $I_{ATP\text{-}P2X7}$ and to determine whether or not $P2X_7R$ alone is sufficient to account for the dose–response curve observed in acinar cells. The resulting $I_{ATP\text{-}P2X7}$ dose–response curve to ATP obtained in Na^+-free, TEA-containing external solution is depicted in Fig. 2 (open squares). The EC_{50} value estimated from Eq. 3 was 59 μM with a Hill coefficient of 4 at +80 mV ($n = 7$). Similarly, the $I_{ATP\text{-}P2X7}$ dose–response curve to ADP performed using 0 Na^+, TEA^+-containing external solutions (Fig. 2, closed symbols) shows that ADP activates I_{ATPCl} in acinar cells (closed circles, $n = 5$) as well as $I_{ATP\text{-}P2X7}$ in HEK-293 cells (closed squares, $n = 8$) with EC_{50} values of 469 and 472 μM and Hill coefficients of 1.7 and 1.8, respectively. Thus, $I_{ATP\text{-}P2X7}$ and I_{ATPCl} are equally sensitive to ADP (472 vs. 469 μM), but $I_{ATP\text{-}P2X7}$ is approximately 2.7-fold more sensitive to ATP than I_{ATPCl} (59 vs. 158 μM). We do not know the reason for this discrepancy, but acinar cells express both $P2X_4$ and $P2X_7$ receptors in an unknown ratio, which could contribute to changes in ATP sensitivity. In addition, higher ectonucleotidase activity in acinar cells compared to HEK-293 cells could contribute to changing the apparent ATP sensitivity of endogenous channels (Henz et al. 2006). Control experiments show that HEK-

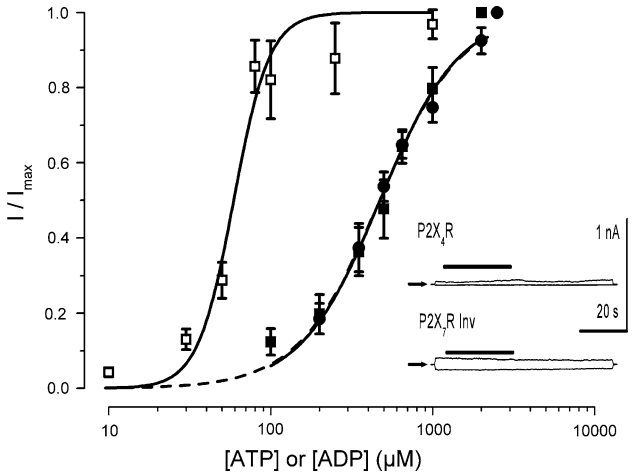

Fig. 2 Dose−response curves for ATP and ADP. Dose–response curves of $P2X_7R$ expressed in HEK cells to ATP (□) or ADP (■) and of I_{ATPCl} recorded from a single acinar cell exposed to ADP (●). *Continuous lines* are fits with Eq. 3 to data; from these fits EC_{50} and Hill coefficients were obtained. These values correspond to 59 μM and 4 (□), 469 μM and 1.7 (■) and 472 μM and 1.8 (●), respectively. Internal solution (in mM): 140 TEACl, 20 EGTA and 20 HEPES (pH 7.3). External solution (in mM): 140 TEACl, 0.5 $CaCl_2$, 100 D-mannitol and 20 HEPES (pH 7.3). *Inset:* Negative controls showing that cells transfected with either $P2X_4R$ or inverted $P2X_7R$ displayed no currents when exposed to 5 mM ATP (bars) in the same conditions used for $P2X_7R$. Zero current level is indicated by *arrows*

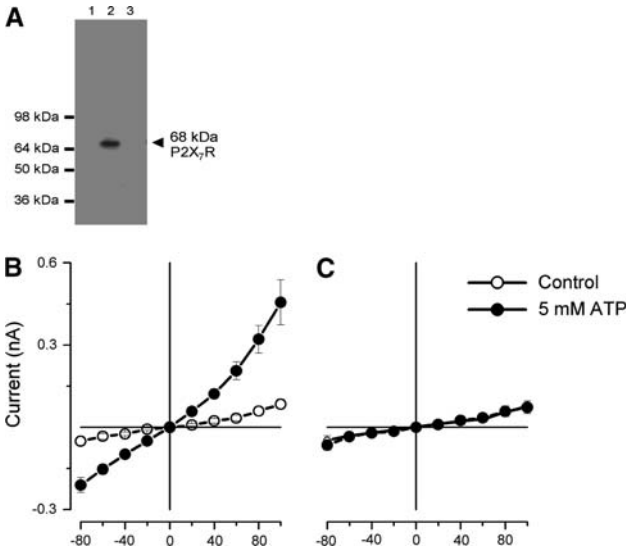

Fig. 3 $P2X_7Rs$ are necessary for I_{ATPCl} generation. Presence of $P2X_7R$ was detected in biotinylated membranes isolated from parotid glands from WT and $P2X_7R^{-/-}$ mice (**A**). Samples were run in a 7.5% SDS-PAGE gel. Lane 1 contains SeeBlue Plus2 Pre-Stained Standard, lane 2 contains membranes from WT mice (50 μg of protein) and lane 3 contains membranes from knockout mice (50 μg of protein). *I–V* relationships were constructed with currents recorded from acinar cells isolated from WT (**B**, $n = 5$) or $P2X_7R^{-/-}$ (**C**, $n = 8$) mice in the absence (*open circles*) or presence (*closed circles*) of 5 mM $(Tris)_2$-ATP. Currents were generated by application of 50-ms voltage steps from −80 to +100 mV in 20-mV increments and then measured near the end of each step. Currents were recorded using an internal solution that contained (in mM) 140 TEACl, 20 EGTA and 20 HEPES (pH 7.3); the external solution contained (in mM) 140 TEACl, 0.5 $CaCl_2$, 100 D-mannitol and 20 HEPES (pH 7.3)

293 cells transfected with either $P2X_4$ or an inverted sequence of $P2X_7$ did not exhibit the ATP-activated current (inset in Fig. 4).

$P2X_7R$ Is Essential for I_{ATPCl} Activation in Parotid Glands

$P2X_7$ receptors appear to be essential for I_{ATPCl} generation in acinar cells (Li et al. 2005). However, our previous data show that I_{ATPCl} was insensitive to block by CB, a known P2X receptor antagonist (Arreola and Melvin 2003). Hence, for completeness, we corroborated the findings of Li and coworkers using mice lacking expression of $P2X_7R$. Figure 3A shows the results of a Western blot for $P2X_7R$ carried out using biotinylated membranes isolated from parotid glands. Lane 1 contains size markers, and lanes 2 and 3 contain membranes isolated from WT and $P2X_7R^{-/-}$ mice, respectively. The 68-kDa band corresponding to $P2X_7R$ was absent in membranes from $P2X_7R^{-/-}$ mice but present in membranes from WT mice. Since $P2X_7R$ is absent in the knockout mouse, we then isolated single parotid acinar cells from WT and $P2X_7R^{-/-}$ mice to functionally analyze the effect of $P2X_7R$ ablation on I_{ATPCl}. Figure 3B demonstrates that extracellular ATP significantly increased the current amplitude (filled circles) above basal levels (open circles) in WT acinar cells at all potentials tested. Both current amplitude and the current–voltage relationship were comparable to those previously reported (Arreola and Melvin 2003). In contrast, I_{ATPCl} was absent in acinar cells from $P2X_7R^{-/-}$ mice (Fig. 3C), thus supporting the idea that $P2X_7R$ is essential for I_{ATPCl} generation.

Na^+ Modulates $P2X_7R$ Anion Permeation

The anion selectivity sequence determined for I_{ATPCl} from reversal potential shifts was $SCN^- > I^- > NO_3^- > Br^- > Cl^-$ > glutamate (Arreola and Melvin 2003). Since our experiments with knockout mice indicated that $P2X_7R$ expression is essential for I_{ATPCl} generation in freshly dissociated acinar cells, we hypothesized that both conductances, I_{ATPCl} and $I_{ATP\text{-}P2X7}$, should display the same or fairly similar anion selectivity sequence. Previous studies in other preparations showed that $P2X_7Rs$ are cation-selective channels with little or no anion permeability (Virginio et al. 1999), yet other studies reported anion permeability in $P2X_7R$-expressing cells (Coutinho-Silva and Persechini 1997; Duan et al. 2003). To quantitatively establish if $P2X_7Rs$ are permeable to both anions and cations, we used the standard GHK equation to analyze

anion substitution experiments (Hille 2001). The GHK equation allowed us to determine the permeability coefficients of TEA^+ and Na^+ relative to Cl^- since TEA^+ and Na^+ are both permeable through P2X$_7$R. Therefore, we independently evaluated P_{TEA}/P_{Cl} and P_{Na}/P_{Cl} ratios from measurements of reversal potential values obtained at various external [TEACl] and [NaCl]. We then used these permeability ratios to determine an anion selectivity sequence from anion substitution experiments, as described in "Materials and Methods."

The relative permeability ratio P_{Na}/P_{Cl} for mouse P2X$_7$R was determined in whole-cell experiments by varying [NaCl] in the external solution and keeping [NaCl] at 140 mM in the pipette solution. P_{TEA}/P_{Cl} was determined in a similar experiment, in which TEACl was used in the bath and pipette solutions instead of NaCl. Figure 4A shows that reduction of both [NaCl] and [TEACl] in the bath shifted the reversal potentials to negative values, which indicates that cationic conductances dominate $I_{ATP\text{-}P2X7}$. The effect of external [NaCl] on the reversal potentials (filled circles) was fit with Eq. 1 (solid line), and a P_{Na}/P_{Cl} value of 220 was obtained. Equally, shifts in reversal potentials obtained using TEACl (open circles) were fit with Eq. 1 to obtain a P_{TEA}/P_{Cl} of 6.17. Hence, P2X$_7$R has significant Cl^- permeability in the presence of TEA^+ but little in the presence of physiologically relevant Na^+ concentrations.

Once P_{TEA}/P_{Cl} was estimated as required by Eq. 2, we proceeded to determine the anion selectivity sequence of P2X$_7$R in cells bathed and dialyzed with solutions containing TEA^+. In these experiments external Cl^- was replaced with equimolar concentrations of SCN^-, I^-, NO_3^-, Br^- or acetate under continuous stimulation with 5 mM ATP(Tris)$_2$. If P2X$_7$R channels are indeed anion-permeable, then the reversal potential of the current activated by external ATP will shift according to the permeability of the anion being tested (Hille 2001). Figure 4 shows a representative time course where both current amplitude at +80 mV and the corresponding reversal potential of the current activated by ATP were continuously monitored in the same cell. Substitution of Cl^- with SCN^-, NO_3^-, I^- and Br^- increased the current amplitude, while acetate decreased it. Cl^- substitution by other anions resulted in a sudden shift in E_r, which was fully reversible upon returning to Cl^-containing medium. This indicates that P2X$_7$Rs display significant anion permeation. Anions that induced larger shifts in reversal potential induced larger outward current amplitude variations, indicating that the anions with the higher permeabilities also have higher conductivities. These results are in complete agreement with the anion permeability of I_{ATPCl} in parotid acinar cells (Arreola and Melvin 2003). Shifts in reversal potential induced by anion substitutions together with the P_{TEA}/P_{Cl} ratio already determined ($P_{TEA}/P_{Cl} = 6.17$, Fig. 4A) and Eq. 2 were then used to estimate apparent permeability ratios for these anions with respect to Cl^-. Table 1 summarizes the apparent anion permeability sequence for P2X$_7$R: $SCN^- > I^- \cong NO_3^- > Br^- > Cl^- >$ acetate. This sequence is identical to that determined in native mouse parotid acinar cells (Arreola and Melvin 2003).

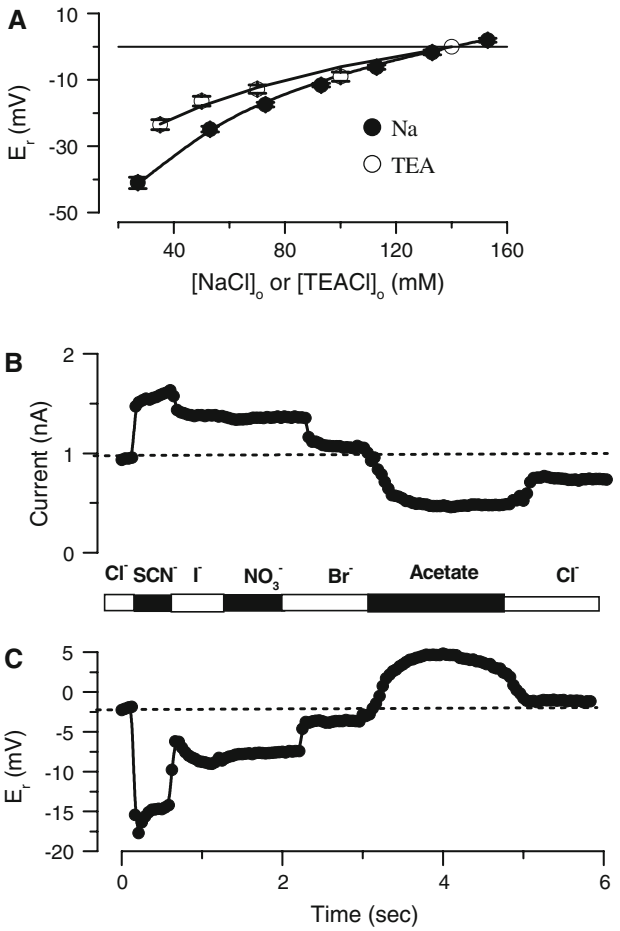

Fig. 4 Anion permeability of $I_{ATP\text{-}P2X7}$. (**A**) The reversal potential of the current activated by 5 mM ATP(Tris)$_2$ was measured in the presence of different external concentrations of NaCl (●, $n = 6$) or TEACl (◯, $n = 8$). The internal solution contained (in mM) NaCl 141 or TEACl 141, EGTA 20 and HEPES 20. The external solution contained (in mM) $CaCl_2$ 0.5, D-mannitol 100, HEPES 20 and TEACl 35, 50, 70, 100 and 140 or NaCl 27, 53, 73, 93, 113, 133 and 153, respectively. *Continuous lines* are fits with Eq. 1 to the data, which gave $P_{TEA}/P_{Cl} = 6.17$ (◯) and $P_{Na}/P_{Cl} = 220$ (●). (**B**) Representative time course ($n = 10$) of current amplitude measured at +80 mV. (**C**) Corresponding time course for reversal potential values ($n = 10$) measured from the current shown in **b**. Current was activated by perfusion of standard external solution (140 mM TEACl) containing 5 mM ATP(Tris)$_2$. Then, in the continuous presence of ATP, Cl^- ions were replaced by 140 mM SCN^-, I^-, NO_3^-, Br^- or acetate (supplied as TEA salts) at the times indicated by the bars. *Dotted lines* indicate the current amplitude or reversal potential levels in the presence of 140 mM Cl^-. Internal solution contained (in mM) EGTA 20, HEPES 20 and TEACl 140; external solutions contained (mM) $CaCl_2$ 0.5, D-mannitol 100, HEPES 20 and TEACl 140

The above data show that P2X$_7$R supports significant anion currents in Na^+-free, TEA^+-containing media. However, as shown in Fig. 4A, the P2X$_7$R conductance in Na^+-based solutions can be totally attributed to Na^+ with negligible Cl^- contribution. The Na^+-dependent modulation of permeation observed in the case of Cl^- could be a phenomenon applicable to other anions too. To test this idea, the external Cl^- was replaced by SCN^- and both the current and reversal potential were determined. Figure 5A, B shows the time course of this response recorded from a representative cell. Time courses at −80 and +80 mV show that SCN^- unexpectedly reduces current amplitude and produces a big change in reversal potential (about −25 mV for this cell), which indicates that SCN^- is highly permeable even in the presence of external Na^+. Despite this, SCN^- has a smaller conductivity in the presence of Na^+ than in the presence of TEA^+. This modulation by Na^+ of anion permeation posed the next question: Is the ion permeability of P2X$_7$ a function of Na^+ concentration? Thus, we performed mole fraction experiments where the external Na^+ was changed while the total monovalent cation concentration (Na^+ + TEA^+) was kept at 140 mM. Figure 5C displays the measured reversal potentials recorded with the mole fraction solutions containing 100% Cl^-. The data can be fit with Eq. 4:

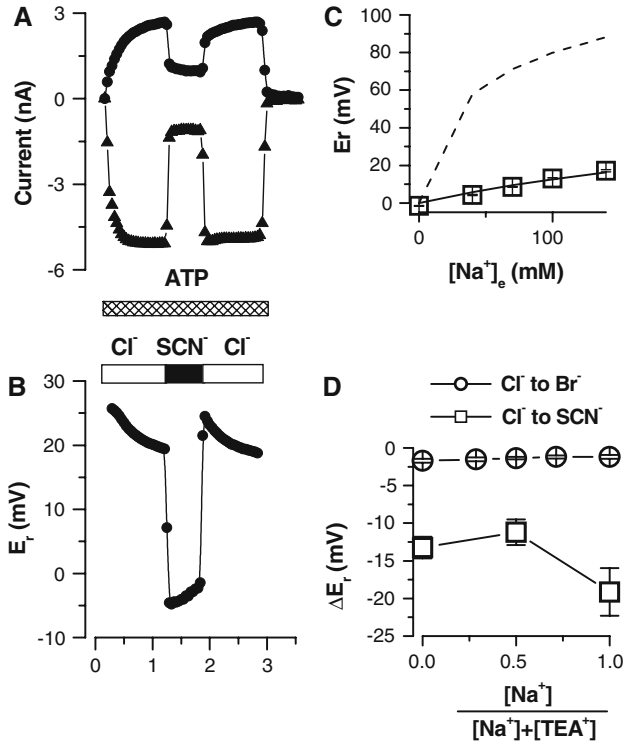

Fig. 5 Na^+-dependent modulation of anion permeability in $I_{ATP\text{-}P2X7}$. (**A**) Representative time course ($n = 5$) of current amplitude measured at +80 mV (◯) or −80 mV (Δ) activated by application of 5 mM ATP(Tris)$_2$ (as indicated by the *striped bar*) in external solutions containing Cl^- or SCN^- supplied as Na^+ salts. (**B**) Corresponding reversal potential time course ($n = 5$) of the current activated by ATP shown in (**A**). (**C**) Reversal potentials of $I_{ATP\text{-}P2X7}$ in the presence of different external [Na^+]. The total concentration of NaCl + TEACl was equal to 140 mM ($n = 4$). Data were fit with Eq. 4 (see text) with a P_{TEA}/P_{Cl} ratio of 3.64 and a P_{Na}/P_{Cl} ratio of 7.7. *Broken line* represents expected reversal potential values for P_{TEA}/P_{Cl} (6.17) and P_{Na}/P_{Cl} (220) plotted against the $[Na]_e$. (**D**) Shift in reversal potential of $I_{ATP\text{-}P2X7}$ (ΔE_r) upon complete substitution of 140 mM Cl^- with Br^- (◯, $n = 4$) or with SCN^- (□, $n = 5$) in the presence of different $Na^+/(Na^+ + TEA^+)$ fractions. Pipette solution was the standard internal solution (140 mM TEACl). Each external mole fraction solution contained Na-*X* and TEA-*X*, where *X* represents either Cl^- or Br^- or SCN^- (concentrations of $CaCl_2$, D-mannitol and HEPES were kept as in the standard external solution). $I_{ATP\text{-}P2X7}$ was activated by 5 mM ATP(Tris)$_2$ in the presence of Cl^- and then switched to Br^- or SCN^-

$$E_r = \frac{RT}{F} \ln \frac{\frac{P_{TEA}}{P_{Cl}}[TEA]_e + \frac{P_{Na}}{P_{Cl}}[Na]_e + [Cl]_i}{\frac{P_{TEA}}{P_{Cl}}[TEA]_i + [Cl]_e} \quad (4)$$

where $[TEA]_e$ represents the external [TEA^+] and $[Na]_e$ represents the external [Na^+]. From this fit (continuous line) a P_{TEA}/P_{Cl} ratio of 3.64 and a P_{Na}/P_{Cl} ratio of 7.7 were estimated; these values are smaller than those obtained using either TEA^+ or Na^+ alone. If the ion fluxes are independent, the expected P_{Na}/P_{TEA} value should be around 36; but instead it falls around 2.1. Furthermore, when we plotted the expected reversal potential values assuming independent fluxes ($P_{TEA}/P_{Cl} = 6.17$ and $P_{Na}/P_{Cl} = 220$) against the $[Na]_e$, we saw that the experimental values fall far away (Fig. 5C, broken line). Thus, presumably ions flow in a nonindependent manner. Finally, the effects of external Na^+ on anion permeability were subsequently determined from mole fraction experiments where the external [Cl^-] was replaced with either Br^- or SCN^-. Figure 5D displays the reversal potential shifts induced by replacement with Br^- (open circles) or SCN^- (open squares). Both anions induced clear reversal potential shifts that were comparable to those observed in anion substitution experiments when 140 mM external TEA^+ was present (see Fig. 4 and Table 1). This result demonstrates that in the presence of external Na^+ P2X$_7$R is permeable to Br^- and SCN^-. The shifts induced by these anions were nearly independent of the Na^+ mole fractions. A −11.2-mV shift was induced by SCN^- when a mixture of 50% Na^+ + 50% TEA^+ was used. This shift is equivalent to a P_{SCN}/P_{Cl} = 3.5, calculated as follows:

$$e^{\frac{\Delta E_r}{RT}} = \frac{\frac{P_{TEA}}{P_{Cl}}[TEA]_i + [Cl]_e}{\frac{P_{TEA}}{P_{Cl}}[TEA]_i + \frac{P_{SCN}}{P_{Cl}}[SCN]_e} \quad (5)$$

where $[SCN]_e$ is the external SCN^- concentration (140 mM), $P_{TEA}/P_{Cl} = 3.64$ (Fig. 5D) and ΔE_r is the shift in reversal potential induced by SCN^-. The P_{SCN}/P_{Cl} value is approximately twofold smaller than that obtained in 0 Na^+, TEA^+-containing medium (Table 1).

Pannexin-1 Is Not Involved in Anion Permeation Induced by Activation of $P2X_7R$

The newly discovered Pannexin-1 is a ubiquitous protein that associates with $P2X_7R$. Long stimulation of $P2X_7R$ with ATP results in Pannexin-1 activation, which forms a macropore (Locovei et al. 2007; Pelegrin and Surprenant 2006) permeable to large cations and anions. Therefore, we asked whether the cation and anion permeability described above can be attributed to Pannexin-1. To test this idea, we repeated our experiments in the presence of a supramaximal concentration of CBX (1 mM), a drug that blocks Pannexin-1 with an EC_{50} of 2–4 μM (Pelegrin and Surprenant 2006). Our results show that in Na^+-free, TEA-containing bath solutions the values of $I_{ATP\text{-}P2X7}$ current reversal potential obtained in the presence of different anions were not modified by the presence of 1 mM CBX (Table 1). Thus, under our experimental conditions, the macropores formed by Pannexin-1 are not the pathway for anion permeation.

Na^+ Dependence of $P2X_7R$ Block by CB

The above data show that the permeation and conduction of anions resulting from $P2X_7R$ activation are controlled by external Na^+ as exemplified by the loss of Cl^- permeability and the decrease in SCN^- permeability in Na^+-containing solutions (Figs. 4A and 5C, respectively). Others have previously shown that the rate of uptake of the large dye YO-PRO-1 (Virginio et al. 1999; Jiang et al. 2005) and the increase in $NMDG^+$ permeability through $P2X_7R$ (Jiang et al. 2005) vary inversely with the $[Na^+]_e$. Also, recently "Na^+ memory" has been postulated to explain changes in the permeability of this receptor in parotid gland cells (Li et al. 2005). All these observations suggest that the presence of external Na^+ modulates different functional properties of $P2X_7R$ and may modulate its response to blockers such as CB. This Na^+-dependent modulation may explain the apparent contradiction regarding CB: Our data strongly indicate that both I_{ATPCl} and the Na^+ current activated by ATP in acinar cells are mediated by $P2X_7R$; however, CB did not block I_{ATPCl} but did block the Na^+ current activated by ATP in acinar cells (Arreola and Melvin 2003). Could the external Na^+ also modulate the CB blockade? To investigate this possibility, we constructed for $I_{ATP\text{-}P2X7}$ dose–response curves of the block by CB in the presence of 140 mM $[Na^+]_e$ or 140 mM $[TEA^+]_e$ (0 Na). Our rationale was that CB interacts with an external binding site on $P2X_7R$ to produce its blocking effect. Consequently, if the structure of the receptor in the presence of physiological concentrations of Na^+ is different from that in the presence of TEA^+, then the ability of CB to block the receptor may be compromised in the presence of TEA. Experiments started with an initial ATP stimulus applied in the absence of CB, followed by a 1-min wash period. Subsequently, the desired CB concentration was applied, followed by a second ATP application in the continuous presence of CB. ATP application continued after removal of the blocker to evaluate the reversibility of the blockade. This protocol was repeated with each desired CB concentration. Figure 6A shows the time courses of the current amplitudes recorded at +80 and –80 mV from two representative cells bathed and dialyzed with either Na^+ (upper panel) or TEA^+ (lower panel) and exposed to ATP and ATP+CB. Amplitudes of the response to the first and second ATP stimuli (after CB washout) were similar, and the averaged amplitude was taken as 100% when calculating the percentage of block for different CB concentrations. In the presence of Na^+, 500 μM CB reduced the current amplitude to a similar extent at +80 and −80 mV (about 53%), suggesting that the blocking effect of CB is voltage-independent. Figure 6B shows a dose–response curve to CB obtained in the presence of Na^+ (closed triangles). The percentage of $I_{ATP\text{-}P2X7}$ block vs. [CB] could be readily described by Eq. 3 with an IC_{50} of 17.6 μM and a maximum blockade of 64%. Conversely, concentrations as high as 2.5 mM CB failed to inhibit the current when the experiments were carried out in the presence of TEA^+ (Fig. 6A, lower time course). In fact, the presence of 2.5 mM CB consistently

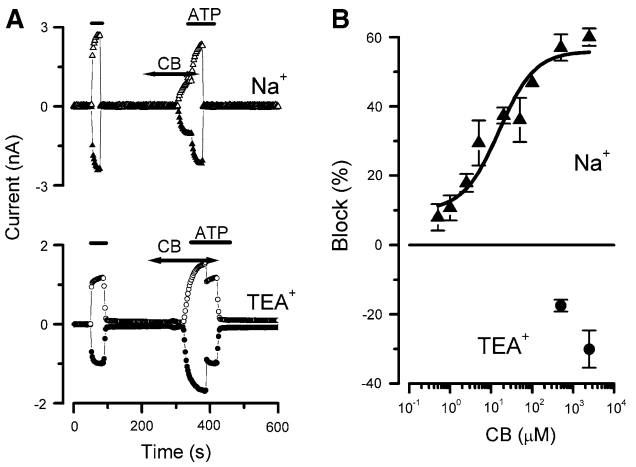

Fig. 6 Block of $I_{ATP\text{-}P2X7}$ by CB is Na^+-dependent. (**A**) Time course of $P2X_7R$ current amplitudes recorded at +80 (*open symbols*) and −80 mV (*filled symbols*) in cells dialyzed and bathed with solutions containing 140 mM NaCl (*triangles, upper panel*) or 140 mM TEACl (*circles, lower panel*). *Black lines* indicate application of 5 mM $ATP(Tris)_2$ and *double-headed arrows* indicate application of 0.5 or 2.5 mM CB (in the presence of Na^+ or TEA^+, respectively). (**B**) Dose–response curve of CB blockade obtained in NaCl (*triangles*) or TEACl conditions (*circles*). Number of cells tested were 4, 4, 5, 4, 3, 5, 2, 7 and 3 for 0.1, 1, 10, 50, 100, 250, 500, 1,000 and 2,500 μM CB, respectively. For the experiments in TEA^+ only two high-concentration data points are plotted: 1,000 ($n = 4$) and 2,500 ($n = 3$). *Continuous line* is the fit with Eq. 3 and yielded an IC_{50} of 17.6 μM with maximum block of 64% and a Hill coefficient = 0.5. Note that CB stimulates $P2X_7R$ currents in cells dialyzed and bathed in Na^+-free solutions containing 140 mM TEA^+ (*filled circles*)

enhanced the current activated by ATP to a similar extent at +80 and −80 mV, and this enhancement was rapidly washed out upon removal of CB (note the drop in current when CB is removed in the presence of ATP). Figure 6B (closed circles) shows that 0.5 and 2.5 mM [CB] enhanced $P2X_7R$ current (current enhancement is represented as negative block % values) at +80 mV by 18 ± 2% ($n = 4$) and 30 ± 5%, respectively ($n = 3$). Thus, our data suggest that when $P2X_7R$ is exposed to an external solution containing TEA^+ and 0 Na^+, the CB binding site is altered by some conformational change in the receptor protein precluding CB blockade.

Discussion

The results presented here and those previously published (Arreola and Melvin 2003) show that I_{ATPCl} and $I_{ATP\text{-}P2X7}$ exhibit similar pharmacology. In acinar cells I_{ATPCl} is activated by Bz-ATP > ATP > ADP; similarly, $I_{ATP\text{-}P2X7}$ in HEK-293 cells is activated by ATP > ADP. Additionally, 5 mM AMP-PNP and ATPγS did activate I_{ATPCl}, while 5 mM CTP induced only partial activation. Other nucleotides and ATP metabolites, such as GTP, UTP, AMP and adenosine, were unable to activate I_{ATPCl}. With the exception of ADP and Bz-ATP, these compounds were not tested on heterologously expressed $P2X_7R$ in this work. However, the ability of the above-mentioned agonists to activate I_{ATPCl} resembles their ability to activate $P2X_7R$ as reported by others (North 2002; Ferrari et al. 1999; Solini et al. 1999; Hugel and Schlichter 2000; Lambrecht 2000; Idzko et al. 2001; Panenka 2001; Budagian et al. 2003; Inoue et al. 2005). Our work also verifies that $P2X_7Rs$ generate I_{ATPCl} in mouse parotid acinar cells since I_{ATPCl} is absent in $P2X_7R^{-/-}$ mice (see also Li et al. 2005).

However, a question remains: Does $P2X_7$ underlie by itself I_{ATPCl}? There are at least two possibilities for the role of $P2X_7R$ in I_{ATPCl} generation. One possibility is that $P2X_7R$ may be part of a multiprotein complex which comprises an anion channel that gains its sensitivity to ATP through $P2X_7R$. In fact, $P2X_7Rs$ have been shown to associate at the molecular level with several proteins, including laminin α_3, integrin β_2, β-actin and α-actinin, among others (Kim et al. 2001); but none of them forms an ion pathway to support ion fluxes. However, prolonged stimulation of $P2X_7R$ with external ATP in Na^+-free solutions is known to induce the formation of "macropores." These macropores allow permeation of large cationic and anionic molecules (up to 900 Da) including $NMDG^+$, TEA^+, YO-PRO, ethidium bromide, anionic Fura-2 and Lucifer yellow (Coutinho-Silva and Persechini 1997; Steinberg et al. 1987; El-Moatassim et al. 1990; Persechini et al. 1998; Di Virgilio et al. 2001). Recently, it has been reported that Pannexin-1—a plasma membrane protein that bears some similarities with the gap junction–forming proteins innexins and connexins—could form large nonselective pores that activate subsequently to $P2X_7R$ stimulation since inhibition of Pannexin-1 prevents the cellular uptake of large molecules (Locovei et al. 2007; Pelegrin and Surprenant 2006). Is Pannexin-1 the anionic pore of I_{ATPCl}? According to our experiments, this does not seem to be the case since the ATP-induced anion permeability was not modified by the presence of 1 mM CBX, a blocker of Pannexin-1. The same concentration of CBX efficiently inhibited the ATP-induced ethidium bromide uptake in HEK-293 cells transfected with mouse $P2X_7R$ (data not shown), indicating that Pannexin-1 was indeed blocked. A second possibility for the role of $P2X_7R$ is that $P2X_7$ itself could grant both ATP sensitivity and anion selectivity to I_{ATPCl}. In other words, after activation with external ATP and in the absence of Na^+ the anions go through the $P2X_7R$ pore. So far, our results support this latter alternative, which was suggested by previous reports (Egan et al. 2006; Ruppelt et al. 2001; Bo et al. 2003; Duan et al. 2003). Thus, the native I_{ATPCl} in mouse parotid acinar cells may reflect the passage of anions through $P2X_7R$, as shown for $P2X_5R$ in developing chick skeletal muscle (Hume and Thomas 1988; Thomas and Hume 1990). This idea is also supported by the data showing that $I_{ATP\text{-}P2X7}$ resulting from the heterologous expression of mouse $P2X_7R$ produces an I_{ATPCl}-like current. Both I_{ATPCl} and $I_{ATP\text{-}P2X7}$ share the same anion selectivity sequence and similar Na^+-dependent actions of CB (see also Arreola and Melvin 2003).

Data presented here show that conductivity and permeation to anions in $P2X_7R$ are both modulated by external Na^+. In the absence of Na^+ $P_{Cl} > 0$ but in Na^+-containing solutions, P_{Cl} was near 0. Morever, P_{SCN}/P_{Cl} was approximately twofold larger in TEA^+ than in Na^+-containing medium, but its conductivity was smaller in Na^+ than in TEA^+. Nevertheless, the anion permeability sequence of $P2X_7R$ determined in the absence of Na^+ was the same as that determined for I_{ATPCl} in native acinar under the same conditions (Arreola and Melvin 2003). In these experiments, reducing the total external salt concentration changed the ionic strength of the solution (but not its tonicity since this was adjusted to ~375 mosm/kg by addition of appropriate amounts of D-mannitol; see "Materials and Methods") and might indirectly alter the apparent ionic conductivity and/or selectivity. However, the same manipulation was used in the Na^+ and TEA^+ experiments, so changing the ionic strength is unlikely to have a major effect on the apparent ionic conductivity and/or selectivity. Although under physiological conditions (with Na^+ present in the external medium) such anionic permeability through $P2X_7R$ would be minimal, this could be important for some critical cellular functions. For example, after ATP stimulation, a small anionic permeability through $P2X_7R$ provides a route for the

release of the neurotransmitter glutamate in native astrocytes (Duan et al. 2003).

In addition, the blockade of $I_{ATP\text{-}P2X7}$ was dependent on external Na^+. When Na^+ was present, $P2X_7R$ was blocked by CB (64% maximum blockade); but when Na^+ was absent, CB, rather than having an inhibitory effect, potentiated $I_{ATP\text{-}P2X7}$. This observation and those previously described indicate that external Na^+ modulates the ability of $P2X_7R$ to interact with CB and anions. This Na^+ dependence of $P2X_7R$ may be explained if the receptor has at least two different conformations. When Na^+ is present, the $P2X_7R$ conformation would have available an external CB binding site outside the electrical field. In the absence of Na^+ and the presence of large cations such as $NMDG^+$ or TEA^+, the $P2X_7R$ would transit to a different conformation—still gated by ATP or ADP—permeable to cations and anions whose conductivity is enhanced by CB. A simple switch from inhibition to enhancement of a drug effect is already suggestive of a structural change in the drug receptor site, and this could also explain why CB blocked the ATP-activated current in parotid acinar cells only when Na^+ was present (Arreola and Melvin 2003). Alternatively, this modulation by Na^+ could be through an allosteric mechanism, as is the case for kainate receptors, which are modulated by Na^+ and Cl^- ions. These receptors have a Cl^- binding site at the dimer interface that stabilizes the structure and allows receptor activation (Plested and Mayer 2007; Plested et al. 2008). Since our data do not provide a mechanistic explanation for $P2X_7R$ modulation by Na^+, this remains an attractive avenue to explore in future work.

In conclusion, this work shows that (1) the $P2X_7R$ is essential for I_{ATPCl} activation in mouse parotid acinar cells; (2) Na^+ regulates anion conductivity and permeation in $P2X_7R$—i.e., in the absence of Na^+ and after stimulation with ATP, the $P2X_7R$ becomes more permeable to anions—(3) Na^+ regulates the effect of CB on $P2X_7R$—i.e., CB inhibits or enhances $P2X_7R$ current in the presence or absence of Na^+, respectively—and (4) in the presence of physiologically relevant Na^+ concentrations, the $P2X_7R$ displays negligible Cl^- permeability.

Acknowledgements We thank Laurie Koek, Jennifer Scantlin, Mark Wagner and Monica Reyna for technical assistance. We also thank Dr. Ted Begenisich for critical reading and comments on this work. This work was supported in part by grants from the National Institutes of Health (DE09692 and DE13539 to J. E. M.), (PO1-HL18208 to RE Waugh), and from CONACyT, Mexico (42561 to J. A.).

References

Arreola J, Melvin JE (2003) A novel chloride conductance activated by extracellular ATP in mouse parotid acinar cells. J Physiol 547:197–208

Arreola J, Melvin JE, Begenisich T (1995) Volume-activated chloride channels in rat parotid acinar cells. J Physiol 484:677–687

Bo X, Jiang LH, Wilson HL, Kim M, Burnstock G, Surprenant A, North RA (2003) Pharmacological and biophysical properties of the human P2X5 receptor. Mol Pharmacol 63:1407–1416

Budagian V, Bulanova E, Brovko L, Orinska Z, Fayad R, Paus R, Bulfone-Paus S (2003) Signaling through P2X7 receptor in human T cells involves p56lck, MAP kinases, and transcription factors AP-1 and NF-kappa B. J Biol Chem 278:1549–1560

Burnstock G (2007) Physiology and pathophysiology of purinergic neurotransmission. Physiol Rev 87:659–797

Coutinho-Silva R, Persechini PM (1997) P2Z purinoceptor-associated pores induced by extracellular ATP in macrophages and J774 cells. Am J Physiol 273:C1793–C1800

Di Virgilio F, Chiozzi P, Ferrari D, Falzoni S, Sanz JM, Morelli A, Torboli M, Bolognesi G, Baricordi OR (2001) Nucleotide receptors: an emerging family of regulatory molecules in blood cells. Blood 97:587–600

Duan S, Anderson CM, Keung EC, Chen Y, Swanson RA (2003) P2X7 receptor-mediated release of excitatory amino acids from astrocytes. J Neurosci 23:1320–1328

Egan TM, Samways DSK, Li Z (2006) Biophysics of P2X receptors. Pfluegers Arch 452:501–512

El-Moatassim C, Mani J, Dornand J (1990) Extracellular ATP^{-4} permeabilizes thymocytes not only to cations but also to low-molecular-weight solutes. Eur J Pharmacol 181:111–118

Evans RL, Bell SM, Schultheis PJ, Shull GE, Melvin JE (1999) Targeted disruption of the *Nhe1* gene prevents muscarinic agonist-induced up-regulation of Na^+/H^+ exchange in mouse parotid acinar cells. J Biol Chem 274:29025–29030

Ferrari D, Stroh C, Schulze-Osthoff K (1999) P2X7/P2Z purinoreceptor-mediated activation of transcription factor NFAT in microglial cells. J Biol Chem 274:13205–13210

Fukushi Y (1999) Heterologous desensitization of muscarinic receptors by P2Z purinoceptors in rat parotid acinar cells. Eur J Pharmacol 364:55–64

Hamill OP, Marty A, Neher E, Sakman B, Sigworth F (1981) Improved patch-clamp techniques for high-resolution current recording from cells and cell-free membrane patches. Pfluegers Arch 391:85–100

Hayashi T, Kawakami M, Sasaki S, Katsumata T, Mori H, Yoshida H, Nakahari T (2005) ATP regulation of ciliary beat frequency in rat tracheal and distal airway epithelium. Exp Physiol 90:535–544

Henz SL, Ribeiro CG, Rosa A, Chiarelli RA, Casali EA, Sarkis JJ (2006) Kinetic characterization of ATP diphosphohydrolase and 5′-nucleotidase activities in cells cultured from submandibular salivary glands of rats. Cell Biol Int 30:214–220

Hernandez-Carballo CY, Perez-Cornejo P, Arreola J (2003) Regulation of volume-sensitive chloride channels by H^+ and Cl^- ions in HEK 293 cells. J Gen Physiol 122:31a

Hille B (2001) Ion channels of excitable membranes. Sinauer Associates, Sunderland, MA

Hugel S, Schlichter R (2000) Presynaptic P2X receptors facilitate inhibitory GABAergic transmission between cultured rat spinal cord dorsal horn neurons. J Neurosci 20:2121–2130

Hume RI, Thomas SA (1988) Multiple actions of adenosine 5′-triphosphate on chick skeletal muscle. J Physiol 406:503–524

Idzko M, Dichmann S, Panther E, Ferrari D, Herouy Y, Virchow C Jr, Luttmann W, Di Virgilio F, Norgauer J (2001) Functional characterization of P2Y and P2X receptors in human eosinophils. J Cell Physiol 188:329–336

Inoue K, Denda M, Tozaki H, Fujishita K, Koizumi S, Inoue K (2005) Characterization of multiple P2X receptors in cultured normal human epidermal keratinocytes. J Invest Dermatol 124:756–763

Jiang LH, Rassendren F, Mackenzie A, Zhang YH, Surprenant A, North RA (2005) *N*-Methyl-D-glucamine and propidium dyes

utilize different permeation pathways at rat P2X7 receptors. Am J Physiol 289:C1295–C1302

Kim M, Jiang LH, Wilson HL, North RA, Surprenant A (2001) Proteomic and functional evidence for a P2X7 receptor signaling complex. EMBO J 20:6347–6358

Lambrecht G (2000) Agonists and antagonists acting at P2X receptors: selectivity profiles and functional implications. Naunyn Schmiedebergs Arch Pharmacol 362:340–350

Leipziger J (2003) Control of epithelial transport via luminal P2 receptors. Am J Physiol 284:F419–F432

Li Q, Luo X, Zeng W, Muallem S (2003) Cell-specific behavior of P2X7 receptors in mouse parotid acinar and duct cells. J Biol Chem 278:47554–47561

Li Q, Luo X, Muallem S (2005) Regulation of the P2X7 receptor permeability to large molecules by extracellular Cl^- and Na^+. J Biol Chem 280:26922–26927

Locovei S, Scemes E, Qiu F, Spray DC, Dahl G (2007) Pannexin1 is part of the pore forming unit of the P2X(7) receptor death complex. FEBS Lett 581:483–488

Ma W, Korngreen A, Weil S, Cohen EB, Priel A, Kuzin L, Silberberg SD (2006) Pore properties and pharmacological features of the P2X receptor channel in airway ciliated cells. J Physiol 571(Pt 3):503–517

McMillan MK, Soltoff SP, Cantley LC, Rudel RA, Talamo BR (1993) Two distinct cytosolic calcium responses to extracellular ATP in rat parotid acinar cells. Br J Pharmacol 108:453–461

Melvin JE, Yule D, Shuttleworth TJ, Begenisich T (2005) Regulation of fluid and electrolyte secretion in salivary gland cells. Annu Rev Physiol 67:445–469

North RA (2002) Molecular physiology of P2X receptors. Physiol Rev 82:1013–1067

North RA, Barnard EA (1997) Nucleotide receptors. Curr Opin Neurobiol 7:346–357

Panenka W, Jijon H, Herx LM, Armstrong JN, Feighan D, Wei T, Yong VW, Ransohoff RM, MacVicar BA (2001) P2X7-like receptor activation in astrocytes increases chemokine monocyte chemoattractant protein-1 expression via mitogen-activated protein kinase. J Neurosci 21:7135–7142

Pelegrin P, Surprenant A (2006) Pannexin-1 mediates large pore formation and interleukin-1beta release by the ATP-gated P2X7 receptor. EMBO J 25:5071–5082

Pérez-Cornejo P, Arreola J (2004) Regulation of Ca^{2+}-activated chloride channels by cAMP and CFTR in parotid acinar cells. Biochem Biophys Res Commun 316:612–617

Persechini PM, Bisaggio RC, Alves-Neto JL, Coutinho-Silva R (1998) Extracellular ATP in the lymphohematopoietic system: P2Z purinoceptors and membrane permeabilization. Braz J Med Biol Res 31:25–34

Plested AJR, Mayer ML (2007) Structure and mechanism of kainate receptor modulation by anions. Neuron 53:829–841

Plested AJ, Vijayan R, Biggin PC, Mayer ML (2008) Molecular basis of kainate receptor modulation by sodium. Neuron 58:720–735

Ralevic V, Burnstock G (1998) Receptors for purines and pyrimidines. Pharmacol Rev 50:413–492

Roman RM, Fitz JG (1999) Emerging roles of purinergic signaling in gastrointestinal epithelial secretion and hepatobiliary function. Gastroenterology 116:964–979

Ruppelt A, Ma W, Borchardt K, Silberberg SD, Soto F (2001) Genomic structure, developmental distribution and functional properties of the chicken $P2X_5$ receptor. J Neurochem 77:1256–1265

Schwiebert EM, Zsembery A (2003) Extracellular ATP as a signaling molecule for epithelial cells. Biochim Biophys Acta 1615:7–32

Solini A, Chiozzi P, Morelli A, Fellin R, Di Virgilio F (1999) Human primary fibroblasts in vitro express a purinergic P2X7 receptor coupled to ion fluxes, microvesicle formation and IL-6 release. J Cell Sci 112:297–305

Solle M, Labasi J, Perregaux DG, Stam E, Petrushova N, Koller BH, Griffiths RJ, Gabel CA (2001) Altered cytokine production in mice lacking P2X7 receptors. J Biol Chem 276:125–132

Steinberg TH, Newman AS, Swanson JA, Silverstein SC (1987) ATP^{4-} permeabilizes the plasma membrane of mouse macrophages to fluorescent dyes. J Biol Chem 262:8884–8888

Tenneti L, Gibbons SJ, Talamo BR (1998) Expression and transsynaptic regulation of $P2X_4$ and P2z receptors for extracellular ATP in parotid acinar cells. J Biol Chem 273:26799–26808

Thomas SA, Hume RI (1990) Permeation of both cations and anions through a single class of ATP-activated ion channels in developing chick skeletal muscle. J Gen Physiol 95:569–590

Turner JT, London LA, Gibbons SJ, Talamo BR (1999) Salivary gland P2 nucleotide receptors. Crit Rev Oral Biol Med 10:210–224

Virginio C, MacKenzie A, North RA, Surprenant A (1999) Kinetics of cell lysis, dye uptake and permeability changes in cells expressing the rat P2X7 receptor. J Physiol 519:335–346

Zeng W, Lee MG, Yan M, Diaz J, Benjamin I, Marino CR, Kopito R, Freedman S, Cotton C, Muallem S, Thomas P (1997) Immuno and functional characterization of CFTR in submandibular and pancreatic acinar and duct cells. Am J Physiol 273:C442–C455